Effect of Tm^{3+} concentration on the emission wavelength shift in Tm^{3+}-doped silica microsphere lasers

ANGZHEN LI,[1] JIQUAN ZHANG,[1] MENG ZHANG,[1] WENHAO LI,[1] SHUNBIN WANG,[1] ELFED LEWIS,[2] GILBERTO BRAMBILLA,[3] AND PENGFEI WANG[1, 4*]

[1]*Key Lab of In-fiber Integrated Optics, Ministry Education of China, Harbin Engineering University, Harbin 150001, China*
[2]*Optical Fibre Sensors Research Centre, Department of Electronic and Computer Engineering, University of Limerick, Limerick, Ireland*
[3]*Optoelectronics Research Centre, University of Southampton, Southampton SO17 1BJ, United Kingdom*
[4]*Key Laboratory of Optoelectronic Devices and Systems of Ministry of Education and Guangdong Province, College of Optoelectronic Engineering, Shenzhen University, Shenzhen, 518060, China*
**Corresponding author: pengfei.wang@dit.ie*

Received XX Month XXXX; revised XX Month, XXXX; accepted XX Month XXXX; posted XX Month XXXX (Doc. ID XXXXX); published XX Month XXXX

In this work, a Tm^{3+}-doped sol-gel silica microsphere lasing at 2.0 μm is reported. Microspheres with different Tm^{3+} concentrations are fabricated by overlaying different Tm^{3+} concentration sol-gel solutions on the surface of a pure silica microsphere resonator and then annealing the sample with a CO_2 laser. Based on a traditional fiber taper-microsphere coupling method, single and multimode microsphere lasing in the wavelength range 1.8-2.0 μm is observed if an 808 nm laser diode is used as a pump source. A relatively low threshold pumping power of 1.2 mW is achieved using this arrangement. This sol-gel method allows for an easy varying of the Tm^{3+} doping concentration. The observed laser output shifts to longer wavelengths when the Tm^{3+} doping concentration increases. This has been explained by the larger Tm absorption at shorter wavelengths. The ability to fabricate sol-gel co-doped silica glass microlasers represents a new generation of low threshold and compact infrared laser sources for use as miniaturized photonic components for a wide range of applications including gas sensing and medical surgery.

OCIS codes: *(140.3460) Lasers; (140.3945) Microcavities; (140.3510) Lasers, fiber.*

Whispering gallery mode (WGM) optical microcavities including microdroplets, microdisks, microspheres and microtoroids have become established as attractive photonic building blocks for use in optoelectronic systems. Devices based on optical microcavities are already considered indispensable for a wide range of applications [1-3]. The combination of high quality factors (up to 10^{10}) and small mode volumes (of the order of 100 μm^3) in WGM resonators significantly enhances light matter interactions, resulting in excellent optical laser cavities with low threshold and narrow linewidth lasers [4-7]. To date, a large number of laser emissions based on rare earth ion doped glass microspheres have been investigated. Yb^{3+}-Er^{3+} co-doped visible microlasers have been widely reported and largely based on glass microsphere resonators [8, 9]. Nd^{3+}-doped and Er^{3+}-doped microsphere resonators have been demonstrated predominantly for emission in the near-infrared range [10, 11].

Tm^{3+}-doped microsphere laser cavities with wavelengths around 2.0 μm have recently attracted much interest owing to their extensive potential applications in laser medicine surgery, military, remote chemical sensing and monitoring of atmospheric pollution. A single mode microsphere laser at 2 μm was demonstrated from a Tm^{3+}-doped tellurite or silica glass microsphere [12, 13]. Tm^{3+}-doped silica microtoroid lasers with a central wavelength of 2 μm fabricated on silicon chips using a sol-gel synthesis process have also been demonstrated [14].

In this work, Tm^{3+}-doped microspheres were prepared using the well-established sol-gel method, which has been verified as a low cost, efficient and flexible method for fabricating many active-ion doped gain microspheres [15, 16]. Infrared lasers with an output central wavelength around 2.0 μm were fabricated and observed by optically coupling the Tm^{3+}-doped microsphere to a silica tapered fiber and using an 808 nm laser diode as pump source. The lasing characteristics were studied in detail by adjusting the coupling position and distance between the tapered fiber and the microsphere. Furthermore, compared with the lasing output at 2 μm only in Ref. [12], the lasing wavelength can be experimentally observed as shifting from 1.83 μm to 2.05 μm when varying the doping concentration in the range 0.05% to 1.5%.

Silica microspheres with diameters ranging from 40 to 200 μm have been fabricated, using standard single-mode fibers (SMF-28,

Thorlabs). These silica microspheres were made in the standard manner using a circular ZnSe lens focused CO_2 laser beam (power ~3 W) which was directed onto a section of a silica single-mode optical fiber. A small weight attached to the bottom of the silica fiber upon heating ensured the formation of a very thin tapered region (diameter circa 3 μm), which acts as the stem of the microsphere. The same CO_2 laser was then used to cut the fiber and to reheat the remaining glass at the tip. The surface tension of the molten silica at the fiber tip under a high temperature caused the fiber tip to assume a spherical shape under the effect of gravity. Finally, a further broad-focus laser heating process was performed to reduce geometric irregularities on the microsphere.

The Tm^{3+}-doped glass was prepared using the well-known sol-gel method [17]. The sol-gel solution was prepared using 6.5 ml tetraethoxysilane (TEOS) in 0.7 ml water and 0.5 ml hydrochloric acid, where 8.3 ml isopropanol acted as the co-solvent. $TmCl_3$ was added to the solution to introduce Tm^{3+} ions. The solution was mixed in a silica beaker and placed on a hotplate, stirred at 70 °C and 400 rpm for 2 hours. This ensured that the Tm^{3+} and ions were evenly dispersed in the solution. Following aging at room temperature for a further 10 h, the solution was ready to use. The undoped microsphere was immersed in the solution for 5 min and the microsphere was coated using the Tm^{3+}-doped solution. Finally, the coated microsphere was heated using a CO_2 laser beam to soften the silica glass (~2000 °C) and hence fabricate the Tm^{3+}-doped microsphere. When heated at this temperature, the organic solvents were completely evaporated and the rare earth ions dissolved into the surface of silica microsphere. This process cycle was repeated 3 times in order to ensure sufficient active ions were introduced into the microsphere. The image of the Tm^{3+}-doped microsphere (with 157 μm diameter) is shown in the inset of Fig. 1.

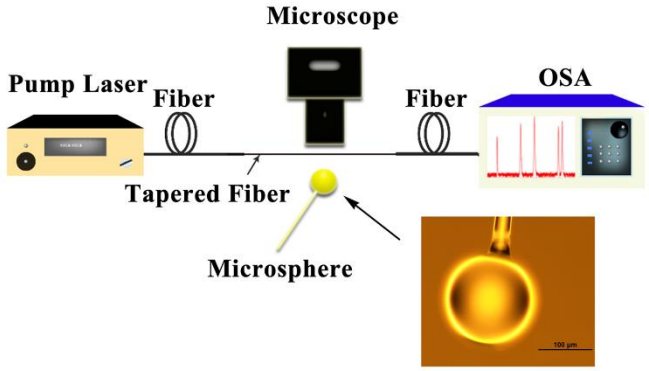

Fig. 1. Experimental setup for characterizing the Tm^{3+}-doped microsphere lasers. Inset: microscope image of the Tm^{3+}-doped microsphere.

The experimental setup for measuring the microsphere laser characteristics is shown in Fig. 1. The tapered fiber used for light coupling was fabricated by heating with a ceramic microheater (CMH-7-19, NTT-AT) a strand of 1060XP single-mode fiber under tension [18]. In this work, the fabrication parameters could be controlled such that the waist diameter of the tapered silica fiber could be accurately controlled in the range 1.0 to 2.0 μm. Light from an 808 nm laser pump diode (LE-LS-808-200TFCS-LH, Leoptics, China) was launched into one end of the taper and then coupled into the microsphere. The transmitted spectrum was collected using an optical spectrum analyzer (OSA) (AQ-6375, Yokogawa, Japan). The coupling positions between the taper and microsphere were monitored from both directions using two 20X microscope objectives which were optically coupled to CCD cameras.

As the position of the microsphere was aligned with the fiber taper, the pump laser light was coupled into the Tm^{3+}-doped microsphere and the resulting 2 μm emission from the microsphere was coupled out of it and transmitted through the fiber taper. The inset of Fig. 2 (a) shows the output optical spectrum from the Tm^{3+}-doped microsphere when the pump power is below the laser threshold. The spectrum was recorded on the OSA with a spectral resolution of 1 nm. When the 808 nm pump laser power reached 1.2 mW, a relatively broad emission in the range 1600 to 2100 nm was observed (In this letter, the meaning of pump power is the input to the fiber taper.). This is the characteristic emission attributed to the $^3F_4 \rightarrow {}^3H_6$ transitions of Tm^{3+} ions as previously reported [19]. As the pump power increased to 7.0 mW, the characteristic multimode laser peaks were observed at 2.0 μm on the OSA with a spectral resolution of 0.05 nm (Fig. 2 (a)). As explained by the schematic of the energy-level diagrams in inset of Fig. 2 (b), Tm^{3+} ions are excited to the $^3H_4$ energy level through the absorption of the 808 nm wavelength light of the pump laser. The depopulation process exists through the rapid non-radiative relaxation from the Tm^{3+}: $^3H_4$ to the $^3F_4$ level and transfer to the $^3H_6$ level with the infrared emission occurring at around 2.0 μm.

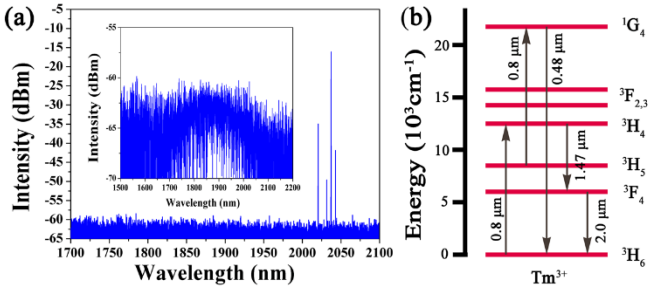

Fig. 2. (a) Laser emission spectra from the Tm^{3+}-doped microsphere when the pump power was set to 7.0 mW. The inset is output spectrum from the Tm^{3+}-doped microsphere excited by an 808 nm laser with a pump power of 1.2 mW. (b) The energy-level diagrams of Tm^{3+} ions and relative transitions.

Changing the position of the coupling between Tm^{3+}-doped microsphere and silica fiber taper, a single mode lasing emission from the microsphere was observed and the resulting output spectrum is shown in Fig. 3 (a). The spectrum was recorded using the same OSA with a spectral resolution of 0.05 nm. The wavelength of the single mode lasing peak is centred at 2037.1 nm, the peak power is 0.028 mW when the pump power reaches 7.0 mW. The output power of the microsphere laser as function of pump power is shown in Fig. 3 (b). Fig. 3 (c) shows the WGMs obtained around 1550 nm, as measured through the fiber taper coupler. The quality factor of the microsphere was measured as high as 10^5 around the wavelength of $\lambda \sim 1550$ nm using the well-known formula $Q=\lambda/FWHM$, where FWHM is the full width at half-maximum. This IR microsphere laser with an output emission at around 2.0 μm and low threshold level is ideal as an integrated optical source for a large

number of applications including gas sensing and surgery in medicine.

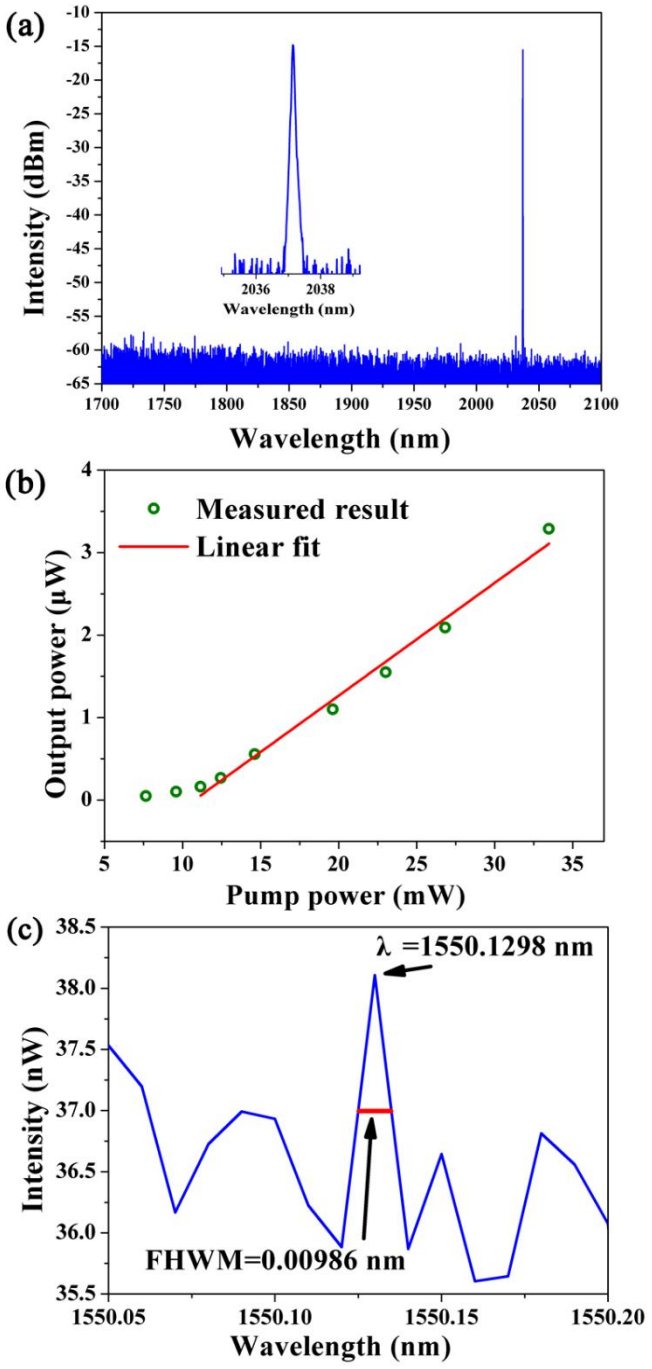

Fig. 3. (a) Single mode laser emission spectrum from the Tm^{3+}-doped microsphere when the pump power reaches 7.0 mW. The inset is the enlargement of the laser peak; (b) Output power of the microsphere laser at 2037.1 nm as a function of pump power. (c) WGMs observed when light is coupled into doped microsphere via the fiber taper coupler.

The characteristic emission attributed to $^3F_4 \rightarrow {}^3H_6$ transitions of Tm^{3+} ions, is observed at around 1.8 μm [20]. Previously, the Tm^{3+}-doped laser was found to have occurred near 2.0 μm. An explanation of the phenomenon that the lasing wavelength at 2.0 μm is a shifted version (by +200 nm) from the emission peak at 1800 nm has been ascribed to the re-absorption in the Tm^{3+} microsphere resulting from two factors: the pumping wavelength is not exactly at the peak of the WGM; and the mode distribution of the 793 nm pump light and 2.0 μm signal light do not exactly match which has been reported in [12]. The sol-gel method is very convenient for ease of changing the doping concentration, and this allowed the characteristics of the Tm^{3+}-doped laser to be investigated with ease for various doping concentrations in the range 0.05 mol% to 1.5 mol%. It was found that the concentration of Tm^{3+} affects the laser emission peak wavelength. In the experiment, the diameter of the sphere was accurately controlled at 150 μm±10 μm. Fig. 4 (a) shows the laser output for the three different Tm^{3+} doping level microspheres when operated with the same pump power. From Fig. 4 (a), it is clear that as the doping concentration of Tm^{3+} increases, the emission position of the laser shifts to longer wavelengths. When the concentrations of Tm^{3+} are 0.05 mol%, 0.1 mol% and 1.5 mol%, the lasers peaks were centred around 1.85 μm, 1.95 μm and 2.05 μm respectively. However the effect of slight geometrical variations on the resonant wavelength can be very important [11, 21, 22]. In the experiment, the effect of different WGM coupling, different microsphere size and different pump power on the emission wavelength shift in Tm^{3+}-doped silica microsphere lasers is demonstrated (with 1.5 mol% concentrations). Fig. 4 (b) shows the laser output for the three different WGM coupling cases when operated with the same microsphere (with 134 μm diameter) and pump power (4.4 mW). Note that some coupling conditions, such as the fiber-sphere air-gap and coupling position may change within the measurements here. The Fig. 4 (c) shows the laser output for the three different pump powers (4.8 mW, 4.2 mW and 5.4 mW) when operated with the same microsphere (with 60 μm diameter). Fig. 4 (d) shows the laser output for the three different microsphere sizes (with 134 μm, 60 μm and 100 μm diameters) when operated with the same pump power. From Fig. 4 (b), (c) and (d), it is clear that different WGM coupling, microsphere size and pump power have effect on the emission wavelength shift. However, these reasons are not enough to account for the observed wavelength shifts from 1.8 μm to 2.0 μm. The absorption and the emission spectra of Tm^{3+} have an overlap over the wavelength of 1.8-2.0 μm. Due to this overlap, high-energy photons may be reabsorbed and then undergo multiple reabsorption and re-emission processes [23, 24]. As the concentration of Tm^{3+} increases, Tm^{3+} ions are in proximity of each other and high-energy photons are more easily reabsorbed. The laser transition of Tm^{3+} is a three-level system, in which the reabsorption of the un-pumped ions in the laser propagation area forces the laser output spectrum to shift to longer wavelengths. This is probably why the emission wavelength of the laser shifts to the wavelength higher value (2.0 μm) as the concentration of Tm^{3+} increases. Actually lasing in the microsphere is rather complex, owing to the large number of high-Q modes that are present in the silica microsphere used in the experiments, the spatial selectivity of the pump source, the loading of the silica microsphere as a result of the fiber taper position, the large spectral gain bandwidth, the variations in the emission and absorption cross sections versus wavelength in the Tm^{3+} doped sol-gel solution materials [25]. Although the mechanism behind the wavelength shifts is much more complex here, it can be primarily justified by the increased contribution of the absorption band at shorter wavelengths (Stokes

shift), which at higher concentrations reduces the gain at shorter wavelengths by increasing the overall losses, thus shifting the emission centre at longer wavelengths.

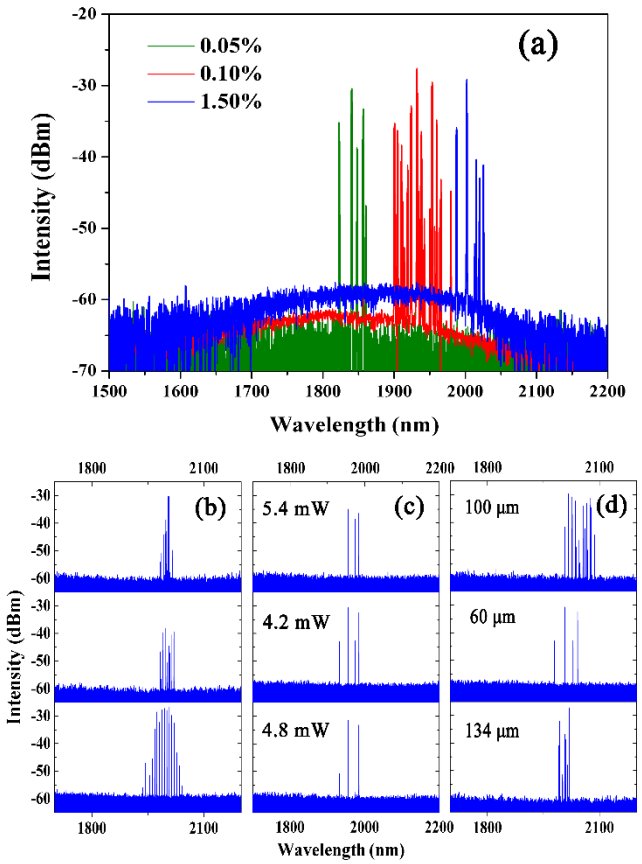

Fig. 4. (a) Laser emission wavelengths with varying Tm^{3+} doping concentrations; (b) Laser emission wavelengths with varying WGM coupling; (c) Laser emission wavelengths with varying pump power; (d) Laser emission wavelengths with varying microsphere size.

In conclusion, Tm^{3+}-doped silica microsphere lasers with emissions around 1.8-2.0 µm in a fiber tapered coupled system has been successfully fabricated and characterized. The source was pumped using a commercial 808 nm laser diode, and this resulted in observable single mode operation of the microsphere at around 2037.1 nm. The threshold pump power could be used as low as 1.2 mW. This Tm^{3+}-doped microsphere resonator therefore provides a low threshold laser source as an integrated optical device for operation in the IR spectral region. This laser is potentially useful for gas sensing, military and medical applications. The sol-gel based fabrication method is low cost, efficient and a highly flexible means of fabricating high gain microspheres as laser sources. It has been shown that the sol-gel method utilized in this study can easily accommodate changing the resulting Tm^{3+} doping concentration. The resulting lasing wavelength also shifts from 1.8-2.0 µm with different doping concentrations. This has been ascribed to the competition between reabsorption and emission, which shifts the lasing emission to longer wavelengths for higher Tm^{3+} ion concentrations.

Acknowledgment.
This work was supported by the National Key R&D Program of China under grant 2016YFE0126500, National Natural Science Foundation of China (NSFC) under grant 61575050, Key Program for Natural Science Foundation of Heilongjiang Province of China under grant ZD2016012, the Open Fund of the State Key Laboratory on Integrated Optoelectronics (Grant no.: IOSKL2016KF03), the 111 project (B13015) at the Harbin Engineering University and by the Fundamental Research Funds of the Central University and the Harbin Engineering University. P. Wang gratefully acknowledges the Recruitment Program for Young Professionals (The Young Thousand Talents Plan); G. Brambilla gratefully acknowledges the Royal Society (London) for his research fellowship.

References

1. L. N. He, S. K. Ozdemir, and L. Yang, Laser Photon. Rev. **7**, 60 (2013).
2. K. J. Vahala, Nature **424**, 839 (2003).
3. S. C. Yang, Y. Wang, and H. D. Sun, Advanced Optical Materials **3**, 1136 (2015).
4. D. W. Vernooy, V. S. Ilchenko, H. Mabuchi, E. W. Streed, and H. J. Kimble, Opt. Lett. **23**, 247 (1998).
5. X. Fan, P. Palinginis, S. Lacey, H. Wang, and M. C. Lonergan, Opt. Lett. **25**, 1600 (2000).
6. M. L. Gorodetsky, A. D. Pryamikov, and V. S. Ilchenko, J. Opt. Soc. Am. B **17**, 1051 (2000).
7. M. L. Gorodetsky, A. A. Savchenkov, and V. S. Ilchenko, Opt. Lett. **21**, 453 (1996).
8. J. A. Valles and R. Galatus, Opt. Mater. **41**, 126 (2015).
9. Y. H. Wang, C. S. Ma, X. Yan, and D. M. Zhang, Opt. Laser Technol. **42**, 336 (2010).
10. Q. L. Li, Y. T. Huang, Y. J. Lin, J. S. Wu, J. Huang, and T. J. Wu, Opt. Commun. **356**, 368 (2015).
11. X. Peng, F. Song, S. B. Jiang, N. Peyghambarian, M. Kuwata-Gonokami, and L. Xu, Appl. Phys. Lett. **82**, 1497 (2003).
12. J. F. Wu, S. B. Jiang, T. Qua, M. Kuwata-Gonokami, and N. Peyghambarian, Appl. Phys. Lett. **87**, 3 (2005).
13. P. Atasi, C. Shu Ying, S. Ranjan, S. Tong, and K. T. V. Grattan, Laser Physics Letters **10**, 085101 (2013).
14. H. Fan, X. Jiang, Y. Ding, and M. Xiao, Sci. China Phys. Mech. **58**, 114204 (2015).
15. L. Yang and K. J. Vahala, Opt. Lett. **28**, 592 (2003).
16. F. Huibo, H. Shiyue, J. Xiaoshun, and X. Min, Laser Physics Letters **10**, 105809 (2013).
17. A. E. Danks, S. R. Hall, and Z. Schnepp, Materials Horizons **3**, 91 (2016).
18. J. M. Ward, A. Maimaiti, V. H. Le, and S. N. Chormaic, Rev. Sci. Instrum. **85**, 10 (2014).
19. B. Richards, A. Jha, Y. Tsang, D. Binks, J. Lousteau, F. Fusari, A. Lagatsky, C. Brown, and W. Sibbett, Laser Physics Letters **7**, 177 (2010).
20. D. A. Simpson, G. W. Baxter, S. F. Collins, W. E. K. Gibbs, W. Blanc, B. Dussardier, and G. Monnom, J. Non·Cryst. Solids **352**, 136 (2006).
21. B. E. Little, J. P. Laine, and H. A. Haus, J. Lightwave Technol. **17**, 704 (1999).
22. G. Palma, M. C. Falconi, F. Starecki, V. Nazabal, T. Yano, T. Kishi, T. Kumagai, and F. Prudenzano, Opt. Express **24**, 26956 (2016).
23. C. W. Hoyt, M. Sheik-Bahae, R. I. Epstein, B. C. Edwards, and J. E. Anderson, Phys. Rev. Lett. **85**, 3600 (2000).
24. R. W. Olson, R. F. Loring, and M. D. Fayer, Appl. Opt. **20**, 2934 (1981).
25. P. Laporta, S. Taccheo, S. Longhi, O. Svelto, and C. Svelto, Optical Materials **11**, 269 (1999).

Full citation listings

1. L. He, Ş. K. Özdemir, and L. Yang, "Whispering gallery microcavity lasers," Laser & Photonics Reviews 7, 60-82 (2013).
2. K. J. Vahala, "Optical microcavities," Nature 424, 839-846 (2003).
3. S. C. Yang, Y. Wang, and H. D. Sun, "Advances and Prospects for Whispering Gallery Mode Microcavities," Advanced Optical Materials 3, 1136-1162 (2015).
4. D. W. Vernooy, V. S. Ilchenko, H. Mabuchi, E. W. Streed, and H. J. Kimble, "High-Q measurements of fused-silica microspheres in the near infrared," Optics Letters 23, 247-249 (1998).
5. X. Fan, P. Palinginis, S. Lacey, H. Wang, and M. C. Lonergan, "Coupling semiconductor nanocrystals to a fused-silica microsphere: a quantum-dot microcavity with extremely high Q factors," Optics Letters 25, 1600-1602 (2000).
6. M. L. Gorodetsky, A. D. Pryamikov, and V. S. Ilchenko, "Rayleigh scattering in high-Q microspheres," Journal of the Optical Society of America B 17, 1051-1057 (2000).
7. M. L. Gorodetsky, A. A. Savchenkov, and V. S. Ilchenko, "Ultimate Q of optical microsphere resonators," Optics Letters 21, 453-455 (1996).
8. J. A. Valles and R. Galatus, "Modeling of Yb^{3+}/Er^{3+}-codoped microring resonators," Optical Materials 41, 126-130 (2015).
9. Y. H. Wang, C. S. Ma, X. Yan, and D. M. Zhang, "Analysis for amplifying characteristics of Er^{3+}-Yb^{3+}-co-doped microring resonators," Optics and Laser Technology 42, 336-340 (2010).
10. Q. L. Li, Y. T. Huang, Y. J. Lin, J. S. Wu, J. Huang, and T. J. Wu, "Ultralow-threshold laser in a Nd^{3+} doped silica microsphere," Optics Communications 356, 368-372 (2015).
11. X. Peng, F. Song, S. B. Jiang, N. Peyghambarian, M. Kuwata-Gonokami, and L. Xu, "Fiber-taper-coupled L-band Er^{3+}-doped tellurite glass microsphere laser," Applied Physics Letters 82, 1497-1499 (2003).
12. J. F. Wu, S. B. Jiang, T. Qua, M. Kuwata-Gonokami, and N. Peyghambarian, "2 μm lasing from highly thulium doped tellurite glass microsphere," Applied Physics Letters 87, 3 (2005).
13. P. Atasi, C. Shu Ying, S. Ranjan, S. Tong, and K. T. V. Grattan, "A high-Q low threshold thulium-doped silica microsphere laser in the 2 μm wavelength region designed for gas sensing applications," Laser Physics Letters 10, 085101 (2013).
14. H. Fan, X. Jiang, Y. Ding, and M. Xiao, "Demonstration of ultralow-threshold 2 micrometer microlasers on chip," Science China Physics, Mechanics & Astronomy 58, 114204 (2015).
15. L. Yang and K. J. Vahala, "Gain functionalization of silica microresonators," Optics Letters 28, 592-594 (2003).
16. F. Huibo, H. Shiyue, J. Xiaoshun, and X. Min, "Demonstration of an erbium-doped microsphere laser on a silicon chip," Laser Physics Letters 10, 105809 (2013).
17. A. E. Danks, S. R. Hall, and Z. Schnepp, "The evolution of 'sol-gel' chemistry as a technique for materials synthesis," Materials Horizons 3, 91-112 (2016).
18. J. M. Ward, A. Maimaiti, V. H. Le, and S. N. Chormaic, "Contributed Review: Optical micro- and nanofiber pulling rig," Review of Scientific Instruments 85, 10 (2014).
19. B. Richards, A. Jha, Y. Tsang, D. Binks, J. Lousteau, F. Fusari, A. Lagatsky, C. Brown, and W. Sibbett, "Tellurite glass lasers operating close to 2 μm," Laser Physics Letters 7, 177-193 (2010).
20. D. A. Simpson, G. W. Baxter, S. F. Collins, W. E. K. Gibbs, W. Blanc, B. Dussardier, and G. Monnom, "Energy transfer up-conversion in Tm^{3+}-doped silica fiber," Journal of Non-Crystalline Solids 352, 136-141 (2006).
21. B. E. Little, J. P. Laine, and H. A. Haus, "Analytic Theory of Coupling from Tapered Fibers and Half-Blocks into Microsphere Resonators," Journal of Lightwave Technology. 17, 704 (1999).
22. G. Palma, M. C. Falconi, F. Starecki, V. Nazabal, T. Yano, T. Kishi, T. Kumagai, and F. Prudenzano, "Novel double step approach for optical sensing via microsphere WGM resonance," Optics Express 24, 26956-26971 (2016).
23. C. W. Hoyt, M. Sheik-Bahae, R. I. Epstein, B. C. Edwards, and J. E. Anderson, "Observation of Anti-Stokes Fluorescence Cooling in Thulium-Doped Glass," Physical Review Letters 85, 3600-3603 (2000).
24. R. W. Olson, R. F. Loring, and M. D. Fayer, "Luminescent solar concentrators and the reabsorption problem," Applied Optics 20, 2934-2940 (1981).
25. P. Laporta, S. Taccheo, S. Longhi, O. Svelto, and C. Svelto, "Erbium-ytterbium microlasers: optical properties and lasing characteristics," Optical Materials 11, 269-288 (1999).